Durability of cantilever inlay-retained fixed dental prosthesis fabricated from multilayered zirconia ceramics with different designs

Ziad N. Al-Dwairi [a,*], Latifah Al-Aghbari [a], Nadin Al-Haj Husain [b,c], Mutlu Özcan [b]

[a] Department of Prosthodontics, Faculty of Dentistry, Jordan University of Science and Technology (JUST), Irbid, Jordan
[b] Division of Dental Biomaterials, Clinic for Reconstructive Dentistry, University of Zurich, Zurich, Switzerland
[c] Department of Reconstructive Dentistry and Gerodontology, School of Dental Medicine, University of Bern, Bern, Switzerland

A B S T R A C T

Purpose: The purpose of this in-vitro study was to investigate the effect of framework design on fracture resistance and failure modes of cantilever inlay-retained fixed partial dentures (IRFDPs) fabricated from two multilayered monolithic zirconia materials.
Materials and methods: Seventy-two natural premolar teeth were prepared as abutments for cantilever IRFDPs using three designs: mesial-occlusal (MO) inlay with short buccal and palatal wings (D1), MO inlay with long palatal wing (D2), MO inlay with long palatal wing and occlusal extension (D3). Full-contoured IRFDPs were fabricated from two monolithic zirconia materials; IPS e.max ZirCAD Prime and Zolid Gen-X. Adhesive surfaces were air-abraded and bonded with MDP-containing resin cement. Specimens were subjected to thermocycling (5–55 °C, 5000 cycles); then, mechanical loading (1.2×10^6 cycles, 49 N). Surviving specimens were loaded until failure in the universal testing machine. All specimens were examined under stereomicroscope, and two samples from each group were evaluated using Scanning Electron Microscope.
Results: Mean failure loads were not significantly different between different framework designs or between two materials. However, IPS e.max ZirCAD Prime showed significantly higher failure rate than Zolid Gen-X during dynamic fatigue (p = 0.009). Samples with D1 design showed higher debonding rate, D2 failed mainly by fracture of the palatal wing and debonding, and D3 failed mainly by fracture of the abutment tooth. Debonded restorations showed mainly mixed failures.
Conclusion: Cantilever IRFDPs with framework designs that maximize adhesion to enamel exhibited promising results. IPS e.max ZirCAD Prime was more susceptible to fractures with the long palatal wing design.

1. Introduction

Replacement of missing teeth is considered an urgent need to restore function and aesthetics. In cases where implant therapy cannot be implemented, conventional fixed partial denture is considered the treatment option of choice to replace single missing teeth (Fugazzotto, 2009). However, full-coverage crown preparation results in removal of approximately 65%−75% sound tooth structure, and may cause pulp injury (Edelhoff and Sorensen, 2002). Therefore, conservative, minimally invasive resin-bonded fixed partial denture (RBFDP) is a recommended alternative particularly with healthy adjacent teeth (Wie et al., 2016).

Inlay-retained fixed partial denture (IRFDP) is a posterior variant of minimally invasive FDPs especially where the adjacent teeth are carious or minimally restored. In such conditions, adaptation of inlay preparation to the lesion extent is carried out to retain a three-unit FDP (Chen et al., 2017). Metal-based IRFDPs showed encouraging clinical results and high success rates of 100% after 4 years and 96.1% after 5 years had been reported (Isidor and Stokholm, 1992; Stokholm and Isidor, 1996). The incorporation of parallel-sided box configurations with frictional retention, and the use of adhesive resin cements were the reasons of the observed increased retention compared to initial IRFDPs (Chaar et al., 2015). Clinical success and favorable long-term results of all-ceramic IRFDPs are related to several factors: material mechanical properties, abutment preparation configuration and retainer design, as well as bonding techniques (Castillo-Oyagüe et al., 2018). Unfortunately, IRFDPs fabricated from lithium disilicate with conventional inlays failed to withstand increased occlusal loads posteriorly and showed high

failure rate of 57% after 5 years 38% after 8 years (Harder et al., 2010). In order to improve clinical performance of all-ceramic IRFDPs, high strength zirconia ceramics had been suggested to replace glass ceramics (Kılıçarslan et al., 2004; Harder et al., 2010). However, high debonding rates and increased chipping complications were reported (Ohlmann et al., 2008; Rathmann et al., 2017). In contrast, excellent survival rate of 95.8% after 5 years of zirconia-based IRFDPs was found when conventional inlay preparation was modified by extracoronal short buccal and lingual wings (Chaar and Kern, 2015). The modified design increased the enamel bonding surface area and offered more favorable stress distribution which minimizes the torsional forces on the retainers when the restoration was loaded non-axially (Wolfartt and Kern, 2006). This was also supported by some in-vitro studies that showed promising results with increased enamel adhesion (Bömicke et al., 2018; Bishti et al., 2019; Samhan and Zaghloul, 2020).

Studies showed superior clinical outcome of single-retainer designs in anterior RBFDPs (Kern and Sasse, 2011; Kern, 2017). Anterior single-retainer RBFDPs exhibited survival rate of 94.4% compared to 73.9% in the double-retainer design after 10 years (Kern and Sasse, 2011). One retrospective study reported 100% survival rate of 35 anterior and posterior cantilever RBFDPs made of lithium disilicate-reinforced and leucite-reinforced glass-ceramics after 6 years (Sailer et al., 2013). It had been assumed that the differential mobility of abutments in the double-retainer design could result in shear and torque stresses which might lead to debonding or fracture of one retainer.

Since chipping of veneering porcelain is a major complication of zirconia-based IRFDPs. The use of more translucent, monolithic zirconia materials might improve the esthetic outcome of IRFDPs without the need for porcelain veneering. With the introduction of multilayer technology, color-gradient as well as strength-gradient zirconia blocks are available. The poly-chromatic color-gradient zirconia block has the same generation of zirconia material with no difference in the flexural strength between base and incisal layers (Kaizer et al., 2020) whereas the strength-gradient material has two generations of zirconia of different flexural strength and translucency at the same zirconia block aiming to merge the advantages of both generations (Michailova et al., 2020). The most recently introduced multilayered color-gradient (4Y-TZP) (Zolid Gen-X, Amann Girrbach) and strength-gradient (3Y-TZP/5Y-TZP) (IPS e. max ZirCAD Prime, Ivoclar) allow fabrication of full-contoured restoration that mimics natural teeth with pigmentation only (Ban, 2021). The possible application of these noval multi-layered zirconia materials in fixed partial dentures could allow fabrication of cantilever IRFPDs to replace missing premolar teeth where high stress bearing capacity is required to withstand posterior loads, and restoration with enhanced esthetics is also essential.

The aim of the present in-vitro study was to investigate the clinical suitability of new high translucent zirconia materials in the fabrication of full-contoured cantilever IRFDPs, and also to provide scientific bases regarding the optimized restoration design that could enhance clinical performance and durability of posterior cantilever IRFDPs. The null hypotheses tested were that the framework design and the material type would have no effect on the fracture resistance of cantilever IRFDPs, and no difference would be found in the failure modes between zirconia materials and different designs.

2. Material and methods

2.1. Experimental model preparation

Seventy-two intact, caries-free recently extracted maxillary premolars were collected from patients in need for extractions for orthodontic treatment (Department of Scientific Research at Jordan University of Science and Technology, Irbid, Jordan; Number: 20210186). Teeth were cleaned with a scalpel and ultrasonic scaler and stored in 0.5% chloramine T solution at room temperature. Samples were first distributed randomly into 3 main groups of 24 specimens each

according to the preparation design as follows: D1 (n = 24): Mesial-occlusal inlay cavity with short buccal and palatal wings. D2 (n = 24): Mesial-occlusal inlay cavity with long palatal wing extended along the whole palatal surface. D3 (n = 24): Mesial-occlusal inlay cavity with long palatal wing and occlusal extension. For each design, cantilever IRFDPs were fabricated from two different multilayered zirconia materials [IPS e.max® ZirCAD® Prime (Ivoclar Vivadent AG, Schaan, Liechtenstein), and Zolid Gen-X (Amann Girrbach AG, Koblach, Austria)] (Fig. 1, Table 1).

Experimental models simulating one abutment tooth, a span of 7 ± 0.2 mm representing missing premolar tooth, and a canine typodont as an adjacent to the prosthesis were used to fabricate IRFDPs. Maxillary plastic model was duplicated into wax replica to be used as reference for setting of teeth at the correct position and relation. An index for teeth was taken using c-silicone (Zetaplus; C-silicone putty, Zhermack, Italy). Premolar roots were covered with duplication silicone material to the level of 2 mm apical to the cement-enamel junction to simulate the physiological periodontal tooth mobility. Roots surfaces were immersed in a duplication silicone (Elite Double 32; Zhermack SpA, Italy) for two times to ensure a thickness of 0.2–0.3 mm representing the natural thickness of the periodontal ligament. Silicone index containing canine and premolar teeth was attached to the vertical rod of the surveyor to be embedded into standard plastic cylinders (35 mm long, and 35 mm diameter) fixed into the surveyor base and filled with epoxy resin. After the final setting of the epoxy resin, models were stored in 0.5% chloramine T solution at room temperature.

2.2. Tooth preparation

Tooth preparation was carried out by one operator with a straight high-speed handpiece fixed to the vertical arm of a parallelometer utilizing water spray coolant. Silicone index (Zetaplus; C-silicone putty, Zhermack, Italy) was used to control the preparation depth of teeth. Inlay preparation was done according to Thompson's guidelines for all-ceramic inlay preparation (Thompson et al., 2010), then modified with wing preparation according to the proposed design (Fig. 2). New burs were used for the preparation of each eight teeth. Occlusal cavity preparation was done following the anatomy of the central fissure with a depth of 1.5 mm, a length of 2 mm, and width of 1.8 mm. Proximal box preparation was done with a width of 3 mm, length of 4 mm, and depth of 1.5 mm with rounded internal angles. The total divergence angle of the proximal inlay walls and the occlusal cavities was 12°. Initial inlay preparation was done using medium grit (75–80 μm) taper round-end diamond bur (SG856/016, Dia-Tessin Dental Diamonds; Vanetti SA,
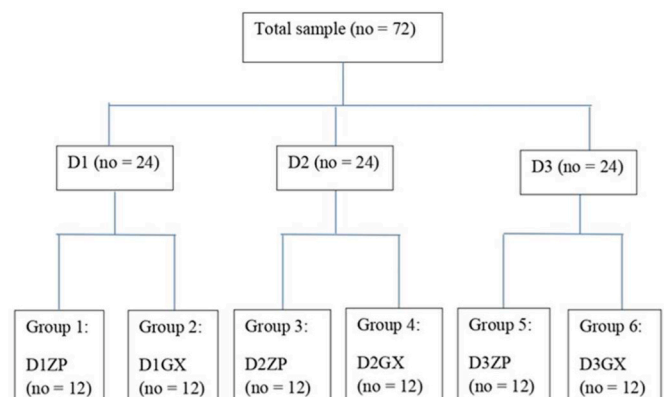

Fig. 1. Specimen distribution according to the preparation design and the fabrication material. D1: Mesial-occlusal (MO) inlay cavity with short buccal and palatal wings. D2: MO inlay cavity with long palatal wing extended along the whole palatal surface. D3: MO inlay cavity with long palatal wing and occlusal extension. ZP: IPS e.max® ZirCAD® Prime. GX: Zolid Gen-X.

Table 1
Preparation designs of retainer abutments.

	Chemical composition (wt%)		Flexural strength (3-point)	E-Modulus	Fracture toughness
IPS e.max ZirCAD Prime rowhead	$ZrO_2+HfO_2+Y_2O_3$.	88–95.5	1200 MPa	No data available	>5 MPa ● m1⁄2
	Y_2O_3	4.5–7			
	HfO_2	≤5			
	Al_2O_3.	≤1			
	Other oxides.	≤1,5			
Zolid Gen-X rowhead	$ZrO_2+HfO_2+Y_2O_3$	≥99	1000 ± 150 MPa	≥200 GPa	No data available
	Y_2O_3	≥6-7			
	HfO_2	≤5			
	Al_2O_3	≤0.5			
	Other oxides.	≤1			

Preparation Design (Dimensions)

a)　Occlusal cavity: 2 mm long, 1.8 mm width, 1.5 mm deep.
　　　Mesial box: 4 mm long, 3 mm wide, 1.5 mm deep
　　　Buccal and palatal wings: 3 mm long, 3 mm height, 0.3-0.5 mm deep

b)　Occlusal cavity: 2 mm long, 1.8 mm width, 1.5 mm deep
　　　Mesial box: 4 mm long, 3 mm wide, 1.5 mm deep
　　　Long palatal wing: extends along the whole palatal surface, 3 mm height, 0.3-0.5 mm deep

c)　Occlusal cavity: 2 mm long, 1.8 mm width, 1.5 mm deep
　　　Mesial box: 4 mm long, 3 mm wide, 1.5 mm deep
　　　Long palatal wing with occlusal extension: extends along the whole palatal surface with
　　　depth of 0.3-0.5 mm, and extends to palatal cusp with 1 mm occlusal reduction

Fig. 2. a-c. Final cantilever IRFDP **a)** D1 design, **b)** D2 design, **c)** D3 design.

Gordevio, Switzerland). Then the preparation was finished using fine grit (35–40 μm) taper round-end diamond bur (SG856/016, Dia-Tessin). Wing preparation was done first using depth preparation bur (SG834/016/6 mm long/medium grit, Dia-Tessin) to create depth orientation groove, and then taper round-end diamond burs. All wings preparation depth was set to 0.3–0.5 mm to remove the maximum bulge of the palatal surface and create a definite path of insertion that was parallel to inlay walls. Dimensions were checked using silicone index with calibrated periodontal probe and electronic digital calliper.

2.3. Framework fabrication

The resin model was scanned using a lab scanner (Ceramill Map 400; Amann Girrbach, Koblach, Austria) to design the IRFDPs using CAD software. A virtual spacer layer of 50 μm was created as clearance for cement thickness. The proximal wing was at least 0.7 mm thick. The minimum connector dimensions were 12 mm² (3 mm width × 4 mm height) with a rounded square intersection. The cantilevered pontic was standardized in all specimens with 7 mm length mesio-distally, 9 mm width bucco-palatally, and 8.5 mm height occluso-gingivally. The pontic had a point-contact with the distal proximal surface of the canine typodont. During nesting, the restoration was centrally positioned within the multilayered blank so as the connector was located within the high strength layer. The frameworks were manufactured from partially sintered monolithic zirconia using five-axis milling machine (ceramill motion 2, Amann Girrbach AG, Koblach, Austria). Half of the cantilevered IRFDPs were fabricated from IPS e.max ZirCAD Prime (Ivoclar Vivadent AG, Schaan, Liechtenstein), and the other half were fabricated from Zolid Gen-X (Amann Girrbach AG, Koblach, Austria). Frameworks were then sintered using a special furnace (Ceramill Therm; Amann Girrbach AG, Koblach, Austria) according to the manufacturers'

sintering protocol (Fig. 2).

2.4. Cementation of IRFDPs

Final prostheses were cleaned with steam and fitted on the abutment teeth. Strength of contact between pontic and the adjacent typodont was assessed using dental floss and all specimens showed the same resistance. Then, flexible silicone gingival mask material (Gingifast; Zhermack SpA, Badia Polesine, Italy) was injected under the cantilevered pontic to represent the gingival soft tissue. Before cementation, fitting surface of zirconia framework was treated by air-abrasion using 50 μm Al_2O_3-powder at 0.2 MPa, at a constant distance of 10 mm for 15 s, and cleaned in an ultrasonic for 5 min with 96% ethanol, then air-dried for 15 s. Double coats of a phosphate containing primer (Z-PRIME™ Plus; BISCO, Schaumburg, USA) were applied to the fitting surface of the restoration directly before cementation and left for 30 s, and then air dried for 10 s and light polymerized with light cure unit for 20 s. The prepared enamel of the abutments was etched with 37% phosphoric acid (DenFil® Etchant-37; Vericom, Anyang, Korea) for 30 s, and then rinsed thoroughly with water spray for 30 s and air dried. Then dual-cure resin cement (Panavia F 2.0; Kuraray Medical Inc., Kurashiki, Japan) was used for cementation of IRFDPs. Cementation was done using custom-device to insure a constant seating pressure of about 1 kg for 10 min. To ensure correct restoration seating during cementation, occlusal index made from autopolymerizing pattern resin (Pattern resin, GC Corp, Tokyo, Japan) was made before the cementation procedure. The luting material was polymerized using photo-poylmerization unit at a distance of 5 mm for 40 s from each side. Thereafter, oxygen protection gel (Oxyguard II, Kuraray) was applied to the margins for 3 min. Excess cement was removed with an explorer. Then, finishing and polishing of the restoration was done with pumice and water.

2.5. Dynamic fatigue and fracture test

After cementation, specimens were stored in distilled water at 37 °C for at least 24 h. Thereafter, they were subjected to thermocycling and mechanical loading. Specimens were thermocycled between 5 °C and 55 °C for 5000 thermal cycles, with a 35 s dwell time at each temperature and transfer time of 10 s. After that, they were exposed to 1,200,000 cycles of dynamic loading using 49 N load at frequency of 1.7 Hz in a computer-controlled dual-axis cyclic loading machine with cross-head descending speed 30 mm s^{-1}. (Power Electronics Co, Amman, Jordan).

After mechanical loading, surviving specimens were loaded until failure in the universal testing machine (WDW-20; Jinan Testing Equipment IE Corporation, Jinan, China). The load was applied vertically on the central point of the occlusal surface of the pontic using a 5-mm-diameter stainless-steel ball at a crosshead speed of 0.5 mm/min until failure occurs. To provide a homogenous force distribution and to avoid primary cracks at the point of loading, a 0.5 mm tin foil was placed between the pontic and the loading ball. The failure loads were determined when a sudden decrease in the applied load occurred and values were recorded in Newten (N).

All specimens were examined using a stereomicroscope (A.KRUSS Optronic GmbH, Germany) with a magnification of × 40 to evaluate mode of failure. failure mode was classified as: I. Fracture of the restoration, II. Fracture of the abutment tooth, III. Failure of the adhesive bond (debonding). Fracture of the restoration was further subcategorized as: I-A. Fracture at the connector, I–B. Fracture of the wing, I–C. Partial fracture of the pontic (crack/minimal), I-D. Complete fracture of the pontic. Debobed failure patterns were categorized into adhesive at the zirconia interface (A1), adhesive at tooth interface (A2), or cohesive in the luting resin (C). Then, two representative debonded samples from each group were further analysed using scanning electron microscope SEM (Quanta FEG 450; FEI, Eindhoven, Netherlands) at different magnifications.

2.6. Statistical analysis

The experimental results were statistically analysed using the two-way analysis of variance test (ANOVA), followed by one-way ANOVA at each level of the study. Fisher Exact test and Mantel-Haenszel test were used for testing the association between proportion of failure during mechanical loading and failure mode with different designs and material types. The level of significance was set at ($p \leq 0.05$). Analytical data calculations were carried out using R statistical computing software version 4.1.

3. Results

3.1. Failures after dynamic fatigue

During mechanical loading, some samples failed to withstand the process of cyclic loading and did not survive until the end of chewing simulation. The highest number of failed samples was found in D1ZP and D2ZP groups (8 out of 12), while D2GX group recorded the lowest failures (2 out of 12) other groups showed failures in the following order: D3ZP (6 out of 12), D1GX (5 out of 12), and D3GX (3 out of 12). The difference in failures during mechanical loading was statistically significant between two materials; IPS e.max ZirCAD Prime zirconia material showed significantly higher chance of failure than Zolid Gen-X ($p = 0.009$). When different groups were compared, significant difference was found only for design D2 ($p = 0.036$). This interaction is illustrated in a histogram in Fig. 3.

3.2. Failure loads

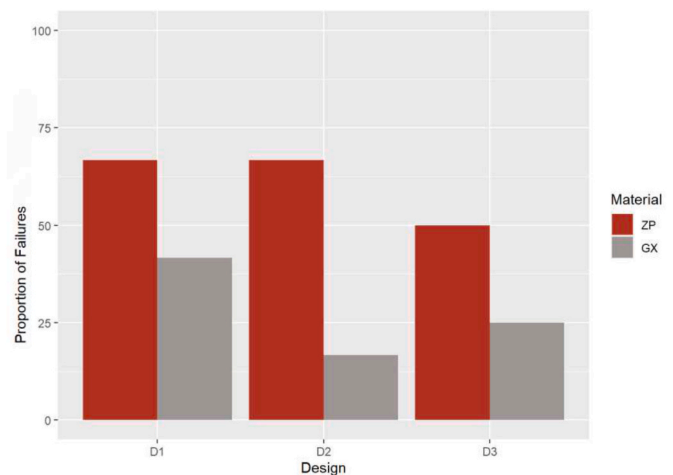Failure load mean values for the surviving samples ranged from 344

Fig. 3. Histogram showing difference of failures during mechanical loading for all groups.

to 1203.2 N. The D2GX group showed the highest fracture load mean (1203.2 ± 1021.0 N), followed by D1ZP (794 ± 951.1 N), D1GX (772 ± 943.2 N), D3GX, (577 ± 327.7 N) and D3ZP (475 ± 87 N). While the lowest fracture load mean of 344.0 ± 84.9 N was for D2ZP. ANOVA test showed no significant difference in fracture loads among different groups (Table 2). Hence, pairwise comparisons test was not needed (Fig. 4).

3.3. Failure mode

Analysis of failure mode showed a significant difference between different designs ($p = 0.000$). Most samples with D1 framework design failed by loss of retention (11/12 in D1ZP, and 10/12 in D1GX), some samples (7/12 in D1ZP, and 2/12 in D1GX) failed by debonding and fracture of the abutment tooth. The palatal cusp and part of the palatal wall were detached with the debonded wing. Samples with D2 design failed mainly by combination of fracture of the long palatal wing and debonding of the inlay (10/12 in D2ZP, and 11/12 in D2GX). While samples with D3 design showed failures of abutment tooth fracture. The palatal wall and palatal cusp were fractured and remained attached to prostheses (11/12 in D3ZP, and 6/12 in D3GX). Failure modes of different designs are shown in Fig. 5. Table 3 represents number of failure patterns for the tested materials with different preparation designs during dynamic fatigue and after fracture test.

Regarding fracture of the restoration, Fisher Exact test showed a significant association between design type and the pattern of restoration fracture ($p = 0.010$). None of the samples fractured at the connector, only one sample in D2GX group had minimal fracture of the pontic, and six samples showed total pontic failure. Fracture of the wing was the highest ($n = 21$) and the majority were with D2 design ($n = 18$).

Evaluation of the debonded restorations showed mainly mixed failures (53.62%). Adhesive failures at the zirconia interface and cohesive failures within the resin cement were the dominant with some areas of adhesive failures at the tooth interface. Other samples showed only

Table 2
Two-way ANOVA results for the effect of different variables on mean fracture load values of IRFDPs.

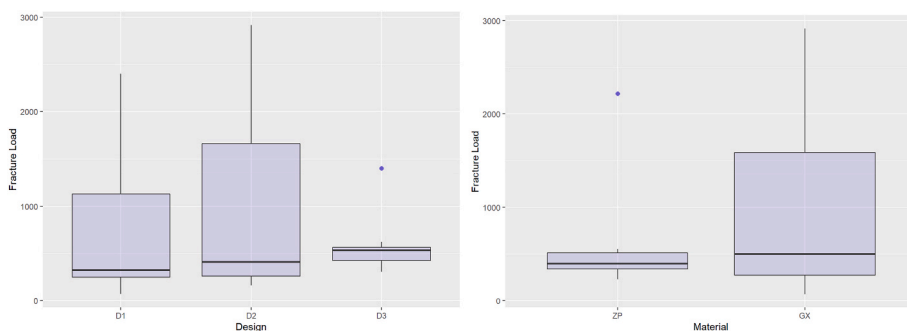| Factor	Df	Sum Sq	Mean Sq	F value	p-value
Design	2	1,298,278.6	649,139.3	1.20	0.3129
Material	1	849,382.3	849,382.3	1.57	0.2183
Design x Material	2	1,298,354.3	649,177.2	1.20	0.3129
Residuals	34	18,353,119.8	539,797.6		

Fig. 4. Boxplots of fracture loads shows no significant differences in the distribution of fracture load means between different designs and materials.
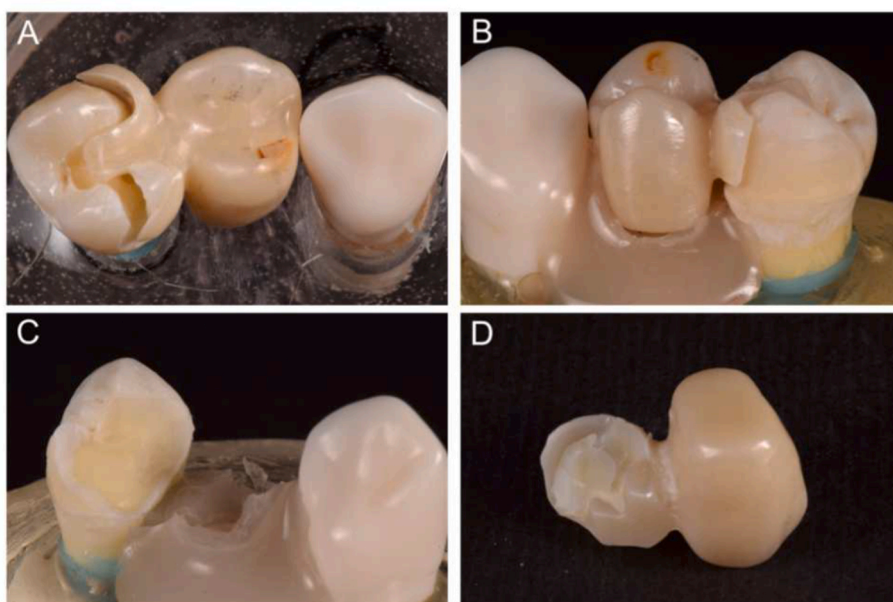

Fig. 5. a-d. Failure modes of different designs. **a)** Debonding and fracture of abutment of D1 design **b)** fracture of the palatal wing and debonding of D2 design **c)** Fracture of the abutment tooth in D3 design **d)** Palatal tooth structure attached to IRFDP in D3 design.

Table 3
Distribution of failure pattern in both materials with different preparation designs.

Failure Mode		During dynamic fatigue						Failure after fracture strength testing					
		GX			ZP			GX			ZP		
		D1	D2	D3	D1	D2	D3	D1	D2	D3	D1	D2	D3
I	I-A	0	0	0	0	0	0	0	0	0	0	0	0
Fracture of the restoration	I–B	0	1	0	0	7	1	0	7	2	0	3	0
	I–C	0	0	0	0	0	0	0	1	0	0	0	0
	I-D	0	0	0	0	0	0	2	2	1	1	0	0
II		4	0	3	0	0	5	2	0	3	2	1	6
Abutment tooth fracture													
III	A1	1	1	1	0	3	4	1	7	3	0	1	1
Failure of the adhesive bond (debonding)	A2	0	0	0	0	0	0	0	0	0	0	0	0
	C	0	0	0	3	0	0	0	0	2	1	1	0
	Mixed	4	1	2	5	5	1	6	2	3	3	2	4

I-A; Fracture of the connector, I–B; Fracture of the wing, I–C; Partial fracture of the pontic (crack/minimal), I-D; Complete fracture of the pontic. A1; Adhesive failure at the cement-framework interface, A2; Adhesive failure at the cement-abutment interface, C; Cohesive failure within the resin cement.

adhesive failures at the zirconia interface (33.33%), or totally cohesive failures (13%). Analysis of representative samples by SEM showed areas of hybrid layer and resin tags indicating adhesive failure at the dentine interface (Fig. 6). Some areas showed flakes or detached lamellae which indicated high stresses inside the resin cement that decreased the cohesive strength of the cement and leads to cohesive failures in the

luting cement (Fig. 6). Other areas showed fracture in the resin cement. The fractured cement surface consists entirely of porous agglomerate that is separated by voids. Only small regions showed areas of smooth cement surface indicated an adhesive failure between tooth structure and resin cement. Evaluation of representative samples indicated mainly a mixed failure in the adhesive bond.
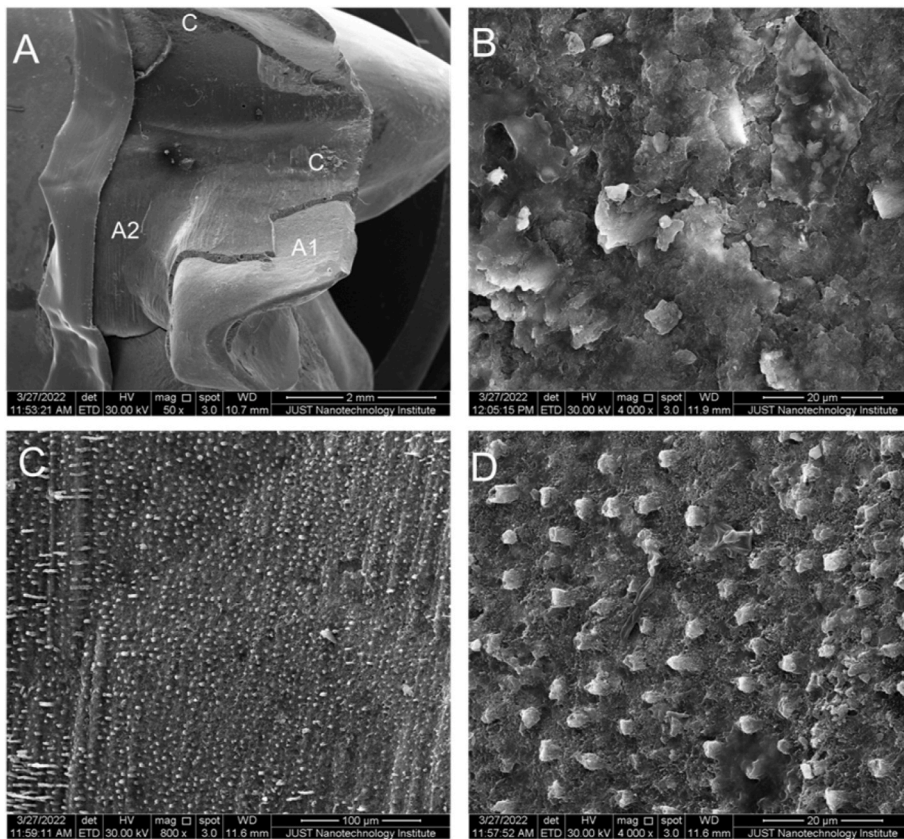
Fig. 6. a-d. SEM micrograph of D1ZP representative sample. **a)** Low magnification exhibited adhesive failure between zirconia and resin cement (A1), adhesive failure between tooth structure and resin cement (A2), and cohesive failure in the resin cement (C) (bar = 2 mm) **b)** High magnification of a cohesive failure region (bar = 20 μm) **c)** Area of adhesive failure between tooth and resin cement (A2) showed the surface of hyprid layer (bar = 100 μm) **d)** Higher magnification of A2 area (bar = 20 μm).

4. Discussion

Resistance of framework to fracture and debonding is the most important parameter for enhanced clinical outcome of all-ceramic adhesive FDPs particularly in posterior region where high occlusal loads increased failure probability (Rathmann et al., 2017). Fracture strength is used to assess the load bearing capacity of new materials and different designs to estimate their success and longevity before they can be recommended for clinical use (Shahin et al., 2014; Gumus et al., 2018). Failure modes analysis is also useful for clinical performance and risk of failures assessment of dental prostheses (Rosentritt et al., 2009).

The maximal masticatory force during function was reported to range from 216 N to 847 N and the highest bite force was recorded in the first molar region (Gibbs et al., 1981, 1986). Studies showed that inlay-retained fixed partial dentures (IRFDPs) require a minimum load of 500 N to resist the mastication forces in the molar region (Ohlmann et al., 2005; Gumus et al., 2018). In the present investigation, failure load means for different groups ranged from 344 N to 1203 N. Most groups found to be able to withstand the required load, while D2ZP and D3ZP groups recorded mean failure loads lower than 500 N. However, they were still within the critical range of the maximal masticatory force range reported in the literature.

Studies evaluated the fracture resistance of zirconia single-retainer IRFDPs with different inlay and wing extension designs reported high failure loads with MOD designs only (Shahin et al., 2014; Bishti et al., 2019). Shahin et al. reported high failure load means of 543.7 N and 746.7 N with MOD designs compared to the other OD inlay designs with lower failure loads ranged from 264 N to 367.3 N regardless of the wing extensions (Shahin et al., 2014). It is worth mentioning that the MOD preparations were more aggressive and less conservative which might affect the fracture resistance of the abutment tooth. Another study recorded a highest median failure load of 204.2 N for the double wing design. Here, the number of wing extension significantly affected

fracture strength, while the inlay depth showed no effect (Bishti et al., 2019). On the other hand, studies evaluated fracture strength of double-retainer IRFDPs made monolithic zirconia reported failure loads between 500 and 2000 N (Bömicke et al., 2018; Gumus et al., 2018; Kermanshah et al., 2020; Samhan and Zaghloul, 2020). However, direct comparison with these studies could be limited due to difference in framework design and lack of dynamic fatigue in some studies.

In the present study, no significant difference in failure loads were found between different groups which indicated that all designs had a comparable fracture resistance with both materials. This could be attributed to the improved mechanical properties of the materials in addition to enhanced resistance form of the restorations and increased enamel adhesion surface area which lead to more favorable stress distribution within the restoration, and minimize torsion forces on the inlay retainers when the restoration is loaded non-axially (Wolfartt and Kern, 2006). These results are consistent with previous studies that found increased fracture strength when preparation design was modified with extracoronal extensions (Bömicke et al., 2018; Samhan and Zaghloul, 2020). In agreement to this, enhanced clinical performance and survival rates of 100% after 20 months and 95.8% after 5 years were reported when modified design was used (Abou Tara et al., 2011; Chaar and Kern, 2015).

The present study showed no significant difference in fracture resistance of strength-gradient (5Y-TZP/3Y-TZP) IPS e.max ZirCAD Prime and color-gradient (4Y-TZP) Zolid Gen-X. These results are consistent with Michailova et al. study that reported comparable strength of molar crowns made of (5Y-TZP/3Y-TZP) IPS e.max ZirCAD Prime and other brands of color-gradient (4Y-TZP) (Michailova et al., 2020). However, the performance of the two tested materials during mechanical loading was significantly different; strength-gradient IPS e.max ZirCAD Prime showed significantly higher failure rate compared to the color-gradient Zolid Gen-X. This could be attributed to differences in lattice structure of the two zirconia generations (5Y-TZP/3Y-TZP) which

could respond differently to stressful loading forces. Repeated or cyclic stresses that causes damage accumulation and progressive microscopic cracks of brittle all-ceramic materials could explain the observed failures of both material (Zhang et al., 2010). In addition to the mechanical stresses, periodic fluctuation in temperature generated by thermocycling and moist environment showed accelerated fatigue of the ceramic material as well as increased hydrolytic degradation of luting cement (Wegner et al., 2002; Lüthy et al., 2006). This would give a more relevant clinical performance of the two materials, thus the color gradient (4Y-TZP) Zolid Gen-X might exhibit better survival and clinical outcome with these particular designs and type of restoration.

Failure mode analysis showed significant difference between different designs; D1 design showed high debonding rate, D2 design failed by debonding and fracture of the palatal wing, and D3 design failed mainly by fracture of the abutment tooth. The increased debonding failures with D1 design could be attributed to the increased amount of dentine to enamel adhesive interface compared to other designs. Also, the design geometry of short wings offered less total surface area for adhesion and lower resistance against different torsional forces on the inlay retainers which leads to higher debonding than other designs. In agreement to these results, Rosentritt et al. reported higher failure rate of debonding in less retentive preparations of anterior cantilever RBFDPs after thermocycling and mechanical loading (Rosentritt et al., 2011). In addition, clinical studies found high debonding rate in IRFDPs with less bonding surface area compared to other preparations in the same study (Ohlmann et al., 2008), and to other studies with modified designs (Chaar and Kern, 2015; Abou Tara et al., 2011).

Fracture of the restoration was mainly found in D2 design where the palatal wing fractured at the area of connection with the proximal inlay. This could be explained by the resistance of the restoration to debonding which resulted in high stress concentration at the inlay-wing connection area as the cantilevered pontic was loaded which resulted finally in fracture of the wing and debonding of the mesial-occlusal inlay. Thompson et al. concluded that ceramic fracture could happen in IRFDPs if retainer didn't debond before the fracture (Thompson et al., 2012). In addition, previous studies explained ceramic fracture that happened at higher loads indicating the increased framework resistance to debonding (Kılıçarslan et al., 2004; Mehl et al., 2010). Although the fracture strength was not significantly different between groups, D2GX specimens presented relatively higher fracture loads (up to 2916 N) and significantly lower failures during chewing simulation.

In the present study connector fracture did not occur in any specimen indicated that the connector was not the weakest part as reported by previous studies investigated zirconia IRFDPs [Kılıçarslan et al., 2004; Shahin et al., 2014; Puschmann et al., 2009]. This disagreement can be attributed to the increased dimensions of the connector (12 mm^2) and the materials high modulus of elasticity and fracture toughness. The wing extensions helped to decrease torsional stresses on the narrow isthmus area and offered more favorable stress distribution (Thompson et al., 2011).

Tooth fracture was mainly found with D3 design in which the whole palatal tooth structure that was bonded to the framework was fractured and detached with the prosthesis. This could be attributed to the enhanced resistance form that resists debonding of the restoration and the increased enamel surface area for adhesion that results in higher adhesive bonding strength. Also, the framework design allowed more stress distribution within the material and decrease the chance of restoration fracture (Thompson et al., 2011). Tooth fracture also could be explained by the presence of inlay preparation with standard dimension regardless of the tooth size which could decrease the overall fracture resistance of the tooth. Tooth fracture also occurred in one sample of D2 design and nine samples of D1 design in which the palatal cusp fractured with the debonded restoration. This could be attributed to increased cusp deflection during dynamic loading which exceeds the debonding stresses on the adhesive interfaces at that area. Other studies also reported teeth fractures during mechanical loading and after

fracture test; resistance of framework to debonding and differences in teeth shapes and composition and response to cyclic loads were supposed to cause such failures (Shahin et al., 2014; Bishti et al., 2019).

In the present study, natural teeth were used as abutment teeth in order to simulate clinical conditions and create an ideal matching of the adhesive interface for IRFDPs. The difference in modulus of elasticity of other alternatives could affect the stress distribution on the restoration and consequently the fracture values (Nawafleh et al., 2016), and the use of metal alloys could lead to overestimation of fracture strength (Mahmood et al., 2011). In addition, resilient periodontal simulation carried out to create more clinically representative failure loads and patterns. Rosentritt et al. found nearly twice increase in fracture loads when minimal mobility of abutment was not allowed (Rosentritt et al., 2011). The adhesive cementation in this study was standardized and the combination of air-abrasion with 50 μm AL_2O_3 at 0.2 MPa and phosphate monomer-containing resin cement was used.

This method has shown enhanced bond durability to zircona surfaces under humid and stressful oral conditions in in-vitro studies and clinical reviews (Kern, 2015; Quigley et al., 2021). In the present study, all debonded samples showed high percentage of mixed (53.62%) and total cohesive failures (13%) indicating that many factors had contributed to such failures rather than the bonding technique by itself and it can be assumed that the cohesive strength of the resin cement was the weakest interface in most cases. In-vitro dynamic fatigue using combined thermocycling and mechanical loading has been found to affect the failure load values of different all-ceramic restorations considerably (Yang et al., 2014). Mechanical loading with 1.2×10^6 cycles and load of 49 N had been proposed to be equivalent to five years clinical service (Rosentritt et al., 2011), and thermocycling of at least 5000 cycles was suggested for resin bond assessment (Özcan and Bernasconi, 2015). Limitations of this study is the lack of a control group using conventional zirconia materials. However, the results of this study were compared to existing literature data. In addition, the exact number of cycles at which failure of each sample had happened during the cyclic loading could not be retrieved.

5. Conclusions

From this study, the following could be concluded:

1. Preparation design that maximizes the adhesion to enamel positively influenced fracture resistance of IRFDPs and different designs showed comparable fracture resistance.
2. Color-gradient zircônia (Zolid Gen-X) showed better performance and significantly lower failure susceptibility compared to strength-gradient zircônia (IPS e.max ZirCAD Prime) particularly with the long palatal wing design.
3. When comparing failure modes between different designs, short buccal and palatal wings showed significantly higher chance of debonding than those of other designs tested, while design with full palatal and occlusal coverage was accompanied with more tooth fracture.

CRediT authorship contribution statement

Ziad N. Al-Dwairi: Writing – review & editing, Writing – original draft, Visualization, Validation, Supervision, Software, Resources, Project administration, Methodology, Investigation, Funding acquisition, Formal analysis, Data curation, Conceptualization. **Latifah Al-Aghbari:** Writing – review & editing, Writing – original draft, Visualization, Validation, Supervision, Software, Resources, Project

administration, Methodology, Investigation, Funding acquisition, Formal analysis, Data curation, Conceptualization. **Nadin Al-Haj Husain:** Writing – original draft. **Mutlu Özcan:** Writing – review & editing, Writing – original draft, Visualization, Validation, Supervision, Software, Resources, Project administration, Methodology, Investigation, Funding acquisition, Formal analysis, Data curation, Conceptualization.

Declaration of competing interest

The authors declare that they have no known competing financial interests or personal relationships that could have appeared to influence the work reported in this paper.

Data availability

No data was used for the research described in the article.

References

Abou Tara, M., Eschbach, S., Wolfart, S., Kern, M., 2011. Zirconia ceramic inlay-retained fixed dental prostheses–first clinical results with a new design. J. Dent. 39, 208–211.

Ban, S., 2021. Classification and properties of dental zirconia as implant fixtures and superstructures. Materials 14, 4879.

Bishti, S., Jäkel, C., Kern, M., Wolfart, S., 2019. Influence of different preparation forms on the loading-bearing capacity of zirconia cantilever FDPs. A laboratory study. J. Prosthodont. Res 63, 347–353.

Bömicke, W., Waldecker, M., Krisam, J., Rammelsberg, P., Rues, S., 2018. In vitro comparison of the load-bearing capacity of ceramic and metal-ceramic resin-bonded fixed dental prostheses in the posterior region. J. Prosthet. Dent 119, 89–96.

Castillo-Oyagüe, R., Sancho-Esper, R., Lynch, C.D., Suárez-García, M.-J., 2018. All-ceramic inlay-retained fixed dental prostheses for replacing posterior missing teeth: a systematic review. J. Prosthodont. Res 62, 10–23.

Chaar, M.S., Kern, M., 2015. Five-year clinical outcome of posterior zirconia ceramic inlay-retained FDPs with a modified design. J. Dent. 43, 1411–1415.

Chaar, M.S., Passia, N., Kern, M., 2015. All-ceramic inlay-retained fixed dental prostheses: an update. Quintessence Int. 46, 781–788.

Chen, J., Cai, H., Suo, L., Xue, Y., Wang, J., Wan, Q., 2017. A systematic review of the survival and complication rates of inlay-retained fixed dental prostheses. J. Dent. 59, 2–10.

Edelhoff, D., Sorensen, J.A., 2002. Tooth structure removal associated with various preparation designs for anterior teeth. J. Prosthet. Dent 87, 503–509.

Fugazzotto, P.A., 2009. Evidence-based decision making: replacement of the single missing tooth. Dent. Clin. 53, 97–129.

Gibbs, C.H., Mahan, P.E., Lundeen, H.C., Brehnan, K., Walsh, E.K., Holbrook, W.B., 1981. Occlusal forces during chewing and swallowing as measured by sound transmission. J. Prosthet. Dent 46, 443–449.

Gibbs, C.H., Mahan, P.E., Mauderli, A., Lundeen, H.C., Walsh, E.K., 1986. Limits of human bite strength. J. Prosthet. Dent 56, 226–229.

Gumus, H.S., Polat, N.T., Yildirim, G., 2018. Evaluation of fracture resistance of inlay-retained fixed partial dentures fabricated with different monolithic zirconia materials. J. Prosthet. Dent 119, 959–964.

Harder, S., Wolfart, S., Eschbach, S., Kern, M., 2010. Eight-year outcome of posterior inlay-retained all-ceramic fixed dental prostheses. J. Dent. 38, 875–881.

Isidor, F., Stokholm, R., 1992. Resin-bonded prostheses for posterior teeth. J. Prosthet. Dent 68, 239–243.

Kaizer, M.R., Kolakarnprasert, N., Rodrigues, C., Chai, H., Zhang, Y., 2020. Probing the interfacial strength of novel multi-layer zirconias. Dent. Mater. 36, 60–67.

Kermanshah, H., Motevasselian, F., Kakhaki, S.A., Özcan, M., 2020. Effect of ceramic material type on the fracture load of inlay-retained and full-coverage fixed dental prostheses. Biomater. Invest. Dent 7, 62–70.

Kern, M., 2015. Bonding to oxide ceramics—laboratory testing versus clinical outcome. Dent. Mater. 31, 8–14.

Kern, M., 2017. Fifteen-year survival of anterior all-ceramic cantilever resin-bonded fixed dental prostheses. J. Dent. 56, 133–135.

Kern, M., Sasse, M., 2011. Ten-year survival of anterior all-ceramic resin-bonded fixed dental prostheses. J. Adhesive Dent. 13, 407.

Kılıçarslan, M.A., Kedici, P.S., Küçükeşmen, H.C., Uludağ, B.C., 2004. In vitro fracture resistance of posterior metal-ceramic and all-ceramic inlay-retained resin-bonded fixed partial dentures. J. Prosthet. Dent 92, 365–370.

Lüthy, H., Loeffel, O., Hammerle, C.H., 2006. Effect of thermocycling on bond strength of luting cements to zirconia ceramic. Dent. Mater. 22, 195–200.

Mahmood, D.J.H., Linderoth, E.H., Vult Von Steyern, P., 2011. The influence of support properties and complexity on fracture strength and fracture mode of all-ceramic fixed dental prostheses. Acta Odontol. Scand. 69, 229–237.

Mehl, C., Ludwig, K., Steiner, M., Kern, M., 2010. Fracture strength of prefabricated all-ceramic posterior inlay-retained fixed dental prostheses. Dent. Mater. 26, 67–75.

Michailova, M., Elsayed, A., Fabel, G., Edelhoff, D., Zylla, I.-M., Stawarczyk, B., 2020. Comparison between novel strength-gradient and color-gradient multilayered zirconia using conventional and high-speed sintering. J. Mech. Behav. Biomed. Mater. 111, 103977.

Nawafleh, N., Hatamleh, M., Elshiyab, S., Mack, F., 2016. Lithium disilicate restorations fatigue testing parameters: a systematic review. J. Prosthodont. 25, 116–126.

Ohlmann, B., Gabbert, O., Schmitter, M., Gilde, H., Rammelsberg, P., 2005. Fracture resistance of the veneering on inlay-retained zirconia ceramic fixed partial dentures. Acta Odontol. Scand. 63, 335–342.

Ohlmann, B., Rammelsberg, P., Schmitter, M., Schwarz, S., Gabbert, O., 2008. All-ceramic inlay-retained fixed partial dentures: preliminary results from a clinical study. J. Dent. 36, 692–696.

Özcan, M., Bernasconi, M., 2015. Adhesion to zirconia used for dental restorations: a systematic review and meta-analysis. J. Adhesive Dent. 17, 7–26.

Puschmann, D., Wolfart, S., Ludwig, K., Kern, M., 2009. Load-bearing capacity of all-ceramic posterior inlay-retained fixed dental prostheses. Eur. J. Oral Sci. 117, 312–318.

Quigley, N.P., Loo, D.S., Choy, C., Ha, W.N., 2021. Clinical efficacy of methods for bonding to zirconia: a systematic review. J. Prosthet. Dent 125, 231–240.

Rathmann, F., Bömicke, W., Rammelsberg, P., Ohlmann, B., 2017. Veneered zirconia inlay-retained fixed dental prostheses: 10-year results from a prospective clinical study. J. Dent. 64, 68–72.

Rosentritt, M., Behr, M., van der Zel, J.M., Feilzer, A.J., 2009a. Approach for valuating the influence of laboratory simulation. Dent. Mater 25, 348–352.

Rosentritt, M., Behr, M., Scharnagl, P., Handel, G., Kolbeck, C., 2011. Influence of resilient support of abutment teeth on fracture resistance of all-ceramic fixed partial dentures: an in vitro study. Int. J. Prosthodont 24, 465–468.

Sailer, I., Bonani, T., Brodbeck, U., Hämmerle, C., 2013. Retrospective clinical study of single-retainer cantilever anterior and posterior glass-ceramic resin-bonded fixed dental prostheses at a mean follow-up of 6 years. Int. J. Prosthodont. (IJP) 26, 443–450.

Samhan, T.M., Zaghloul, H., 2020. Load to failure of three different monolithic zirconia inlay-retained fixed dental prosthesis designs with three surface treatments. Braz. Dent. Sci 23, 10.

Shahin, R., Tannous, F., Kern, M., 2014. Inlay-retained cantilever fixed dental prostheses to substitute a single premolar: impact of zirconia framework design after dynamic loading. Eur. J. Oral Sci. 122, 310–316.

Stokholm, R., Isidor, F., 1996. Resin-bonded inlay retainer prostheses for posterior teeth, A 5-year clinical study. Int. J. Prosthod. 9, 161–166.

Thompson, M., Thompson, K., Swain, M., 2010. The all-ceramic, inlay supported fixed partial denture. Part 1. Ceramic inlay preparation design: a literature review. Aust. Dent. J. 55, 120–127.

Thompson, M., Field, C., Swain, M., 2011. The all-ceramic, inlay supported fixed partial denture. Part 2. Fixed partial denture design: a finite element analysis. Aust. Dent. J. 56, 302–311.

Thompson, M., Field, C., Swain, M., 2012. The all-ceramic, inlay supported fixed partial denture. Part 3. Experimental approach for validating the finite element analysis. Aust. Dent. J. 57, 23–30.

Wegner, S.M., Gerdes, W., Kern, M., 2002. 4 Effect of different artificial aging conditions on ceramic-composite bond strength. Int. J. Prosthodont. (IJP) 2002 (15), 267–272.

Wie, Y.-R., Wang, X.-D., Zhang, Q., Li, X.-X., Blatz, M.B., Jian, Y.-T., et al., 2016. Clinical performance of anterior resin-bonded fixed dental prostheses with different framework designs: a systematic review and meta-analysis. J. Dent. 47, 1–7.

Wolfartt, S., Kern, M., 2006. A new design for all-ceramic inlay-retained fixed partial dentures: a report of 2 cases. Quintessence Int. 37, 27–33.

Yang, R., Arola, D., Han, Z., Zhang, X., 2014. A comparison of the fracture resistance of three machinable ceramics after thermal and mechanical fatigue. J. Prosthet. Dent 112, 878–885.

Zhang, L., Wang, Z., Chen, J., Zhou, W., Zhang, S., 2010. Probabilistic fatigue analysis of all-ceramic crowns based on the finite element method. J. Biomech. 43, 2321–2326.